

ACCEPTED TO THE A.J.

Preprint typeset using L^AT_EX style emulateapj v. 04/03/99

THE KPNO INTERNATIONAL SPECTROSCOPIC SURVEY.
I. DESCRIPTION OF THE SURVEY

JOHN J. SALZER^{1,2} AND CARYL GRONWALL^{1,3}Astronomy Department, Wesleyan University, Middletown, CT 06459; slaz@astro.wesleyan.edu,
caryl@adcam.pha.jhu.eduVALENTIN A. LIPOVETSKY^{1,4} AND ALEXEI KNIAZEV¹Special Astrophysical Observatory, Russian Academy of Sciences, Nizhny Arkhyz,
Karachai-Circassia 357147, Russia; aka@sao.ru

J. WARD MOODY

Department of Physics & Astronomy, Brigham Young University, Provo, UT 84602;
jmoody@astro.byu.edu

TODD A. BOROSON

U.S. Gemini Program, National Optical Astronomy Obs., P.O. Box 26732, Tucson, AZ 85726;
tyb@noao.edu

TRINH X. THUAN

Astronomy Department, University of Virginia, Charlottesville, VA 22903;
txt@starburst.astro.virginia.edu

YURI I. IZOTOV

Main Astronomical Observatory, National Academy of Sciences of Ukraine, Goloseevo, Kiev 03680,
Ukraine; izotov@mao.kiev.ua

JOSE L. HERRERO

BBN Technologies, Cambridge, MA 02140; jose@world.std.com

LISA M. FRATTARE¹

Space Telescope Science Institute, Baltimore, MD 21218; frattare@stsci.edu

Accepted to the A.J.

ABSTRACT

The KPNO International Spectroscopic Survey (KISS) is a new objective-prism survey for extragalactic emission-line objects. It combines many of the features of previous slitless spectroscopic surveys that were carried out with Schmidt telescopes using photographic plates with the advantages of modern CCD detectors. It is the first purely digital objective-prism survey, and extends previous photographic surveys to substantially fainter flux limits. In this, the first paper in the series, we give an overview of the survey technique, describe our data processing procedures, and present examples of the types of objects found by KISS. Our first H α -selected survey list detects objects at the rate of 18.1 per square degree, which is 181 times higher than the surface density of the Markarian survey. Since the sample is line-selected, there is an imposed redshift limit of $z \lesssim 0.095$ due to the filter employed for the objective-prism observations. We evaluate the quality of the observed parameters derived from the survey data, which include accurate astrometry, photometry, redshifts, and line fluxes. Finally, we describe some of the many applications the KISS database will have for addressing specific questions in extragalactic astronomy. Subsequent papers in this series will present our survey lists of emission-line galaxy candidates.

Subject headings: galaxies: emission-lines — galaxies: Seyfert — galaxies: starburst — surveys

¹Visiting Astronomer, Kitt Peak National Observatory. KPNO is operated by AURA, Inc. under contract to the National Science Foundation.

²NSF Presidential Faculty Fellow.

³present address: Department of Physics & Astronomy, Johns Hopkins University, Baltimore, MD 21218.

⁴Deceased 22 September 1996.

1. INTRODUCTION

Active galactic nuclei (AGN) and galaxian starbursts are among the most energetic phenomena known in the universe. From Blue Compact Dwarf galaxies to QSOs, galaxian activity manifests itself on all scales and over the entire range of the electromagnetic spectrum. Activity in galaxies appears to be common, with between 5 and 10% of all galaxies showing evidence for it via the presence of unusually strong emission lines in their spectra (e.g., Salzer 1989, Gregory *et al.* 2000). The study of these objects has been a major research topic for many years, and a great deal has been learned about the physical processes occurring in the active regions of both AGN and starburst galaxies. Much still remains to be understood. How does the activity, be it central or global, shape the overall evolution of the host galaxy? Do all galaxies cycle through periods of activity? What role does environment play in whether or not a galaxy becomes active? Given that many of the galaxies we observe at high redshift are active, can we understand their evolutionary status in the context of what we observe locally? How has the global star formation density evolved as a function of cosmic epoch?

Central to the study of AGN and starburst activity have been the surveys which have cataloged large samples for subsequent investigation. Few types of extragalactic surveys have been as scientifically fruitful as the various objective-prism surveys for UV-excess and emission-line galaxies (ELGs) carried out with Schmidt telescopes. Much of what we know about Seyfert galaxies, starburst galaxies, and even QSOs has been learned by studying objects originally discovered in surveys with such familiar names as the Markarian, Tololo, Wasilewski, Michigan (UM), Kiso, Case, and Second Byurakan (SBS) surveys.

Virtually all of the existing surveys for galaxies which display some form of unusual activity (e.g., blue colors or strong emission lines) have been carried out using Schmidt telescopes and one of three detection methods. The first, which is commonly referred to as the color-selection technique, uses multiple exposures taken through two or three filters to isolate the bluest galaxies. This method has been used by Haro (1956), Takase & Miyauchi-Isobe (1993; Kiso survey), and Coziol *et al.* (1993, 1997; Montreal survey). The well known Palomar-Green survey (Green *et al.* 1986; PG survey) for UV-bright stars and QSOs also employed this technique. The other two methods employ objective prisms. One, the UV-excess technique, was pioneered by Markarian (1967) and Markarian *et al.* (1981). It is similar to the color-selection method in that the criterion for inclusion is the presence of a very blue continuum. The other

selects objects via the presence of emission lines in the objective-prism spectra. Surveys of this type include the Tololo (Smith 1975, Smith *et al.* 1976), Michigan (UM, MacAlpine *et al.* 1977, MacAlpine & Williams 1981), Wasilewski (1983), and Universidad Complutense de Madrid (UCM, Zamorano *et al.* 1994, 1996; Alonso *et al.* 1999) surveys. Finally, the Case (Pesch & Sanduleak 1983, Stephenson *et al.* 1992) and Second Byurakan surveys (Markarian *et al.* 1983, Markarian & Stepanian 1983, Stepanian 1994) use a hybrid scheme, selecting galaxies based on both UV excess and line emission.

In recent years various observatories have begun experimenting with the use of CCD detectors on Schmidt telescopes. While CCDs had become the detector of choice for most observing applications by the mid-1980's, photographic plates have remained in use on Schmidt telescopes due to their vastly superior areal coverage. However, the advent of large format CCDs (2048×2048 pixels and larger) now provides sufficiently large fields-of-view (in excess of one degree square) that it has become advantageous to carry out a variety of wide-field survey projects using CCDs on Schmidt telescopes (Armandroff 1995). These advances have motivated us to initiate a new survey for emission-line galaxies.

Our new survey is called KISS - the KPNO International Spectroscopic Survey. The technique we employ combines the benefits of a traditional photographic objective-prism survey with the advantages of using a CCD detector, and represents the **next generation of wide-field objective-prism surveys**. The goal of the KISS project is to survey a large area of the sky for extragalactic emission-line sources, and to reach a minimum of two magnitudes deeper than any of the previous line-selected Schmidt surveys. Our initial plan was to be able to detect strong-lined ELGs with continuum magnitudes down to $B = 20 - 21$, and to be complete to $B = 19 - 20$. The use of a CCD detector allows us to achieve these goals.

We stress that the need for this type of survey goes beyond the desire to simply find **more** AGN and starburst galaxies. The type of scientific questions we wish to address requires large samples with well defined selection criteria and completeness limits. Our research cuts across the traditional lines of study of active galaxies, and touches upon nearly all areas of extragalactic astronomy, such as galaxy formation and evolution, chemical evolution, and large-scale structure and cosmology. Although we fully expect to discover many new objects which possess noteworthy characteristics that will warrant individual study, the prime motivation for this survey is to create a sample of objects that can be used as probes

for studying more general questions. We will discuss some of these applications of the KISS sample of galaxies in Section 5.

In the next section we describe in detail our instrumental setup and observational technique, while Section 3 gives an overview of our image processing and analysis software which is central to the survey effort. Section 4 presents the results from our first two survey lists, evaluates the quality of the survey data (e.g., photometry, astrometry, redshifts), and gives a preliminary analysis of the survey contents. In Section 5 we list some of the possible uses of the KISS sample for attacking specific problems relevant to extragalactic astronomy and cosmology. Finally, Section 6 summarizes our results.

2. OBSERVATIONS

2.1. *Instrumentation*

All survey data were acquired using the 0.61-meter Burrell Schmidt telescope⁵ located on Kitt Peak. During the observations of the first survey strip, the detector used was a 2048×2048 pixel STIS CCD (S2KA). This CCD has $21\text{-}\mu\text{m}$ pixels, which yielded an image scale of $2.03 \text{ arcsec/pixel}$. The overall field-of-view was $69 \times 69 \text{ arcmin}$, and each image covered $1.32 \text{ square degrees}$. The CCD was illuminated fairly evenly by the telescope, although the slightly undersized Newtonian secondary mirror introduced modest vignetting (10–15%) on the edges of the images.

The spectral data were taken with two separate prisms installed on the top ring of the telescope, in front of the corrector plate. Data taken in the blue portion of the spectrum utilized a 2° prism, which gave spectra with a reciprocal dispersion of 19 \AA/pixel at 5000 \AA . The red survey spectral data were obtained with a 4° prism, which provided a reciprocal dispersion of 24 \AA/pixel at $\text{H}\alpha$. Thus, the two sets of spectral data have roughly the same spectral resolution.

During the planning stages for the survey, it was deemed essential to restrict the wavelength range covered by the objective-prism spectra. Although traditional objective-prism surveys typically did not employ filters, there are two primary reasons why it is important for our CCD-based survey. First, CCDs are more-nearly panchromatic detectors than are photographic plates. For example, the IIIa-J emulsion used for many of the previous photographic surveys has a sensitivity cutoff above 5350 \AA , effectively limiting the length of each spectrum on the red side. No such cutoff exists for CCDs. Second, and more important for the present survey, is the depth to which CCDs can reach relative to photo-

graphic plates. Since our CCD can detect continua in objects as faint as $B = 20 - 21$, the problem of image crowding and overlap becomes enormous. An unfiltered image taken with the 2° prism yields spectra that are ~ 250 pixels long! With typically $4000 - 10,000$ objects per image, essentially every spectrum is overlapped by another. For the photographic surveys, which rarely detected the continuum in objects fainter than $B = 17$ or 18 , spectral overlap was not as severe a problem.

Therefore, two specially designed filters were used for the KISS observations in order to restrict the wavelength range of the spectra. The filter for the blue spectral survey was designed to cover the wavelength range from just below restframe $\text{H}\beta$ up to, but not including, the strong $[\text{O I}]\lambda 5577$ night sky line. The decision to exclude the night sky $[\text{O I}]$ line was based in large part on our desire to keep the sky background as low as possible. Since in a slitless spectroscopic survey like KISS, every pixel of the detector is illuminated by the night sky spectrum *at all wavelengths*, the sky background can pose a serious limitation on the depth of the survey data. Hence, eliminating the bright $[\text{O I}]$ line results in a substantial reduction in the background flux. The region covered by our blue filter (see Figure 1a), $4800 - 5520 \text{ \AA}$, is one of the darkest portions of the night sky spectrum. The red spectral filter (Figure 1b), was likewise chosen to have a blue limit just below restframe $\text{H}\alpha$, and to extend up to the beginning of a strong OH molecular band near 7200 \AA . In both cases, the primary emission line we are sensitive to ($[\text{O III}]\lambda 5007$ in the case of the blue survey, and $\text{H}\alpha$ for the red survey) is detectable up to a redshift of approximately 0.095.

2.2. *The Observational Data*

Three types of images are obtained for the survey. The data for each survey field consists of direct images acquired through Harris B and V filters (which closely mimic standard Johnson B and V filters), spectral images in one or both of the spectral regions mentioned above and taken through the relevant prism and spectral filter combination, and a pair of short exposure calibration images. Examples of a direct and spectral image for a portion of one KISS field are shown in Figures 2 and 3, respectively.

Direct Images. Roughly 30% of the survey observing time is spent in direct imaging mode, i.e., with no prism on the telescope. For each field in the survey, we obtain direct images through two filters (B and V) to a depth of 1 to 2 magnitudes fainter than the limiting magnitude of the spectral images. This is done for several reasons:

⁵Observations made with the Burrell Schmidt of the Warner and Swasey Observatory, Case Western Reserve University. Prior to 1997 October, the Burrell Schmidt was operated jointly by CWRU and KPNO.

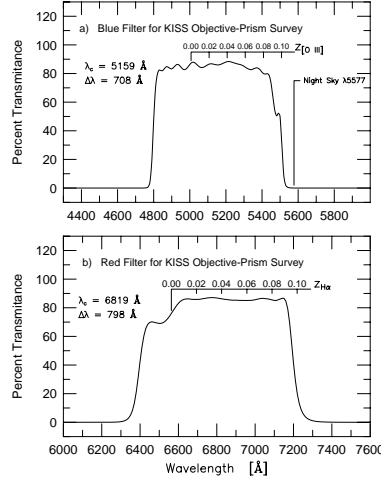


FIG. 1.— Filter throughput tracings for the filters used in the KISS project. (a) The blue survey ([O III] selected) filter. (b) The red survey (H α selected) filter. The central wavelengths (λ_c) and widths at 50% throughput ($\Delta\lambda$) are listed for both filters. The scale above the tracings shows the approximate location of the relevant emission line for the redshifts indicated. Both filters are sensitive to their primary emission line out to redshifts of $z \approx 0.095$. In addition, the blue filter is sensitive to H β emission out to $z \approx 0.13$.

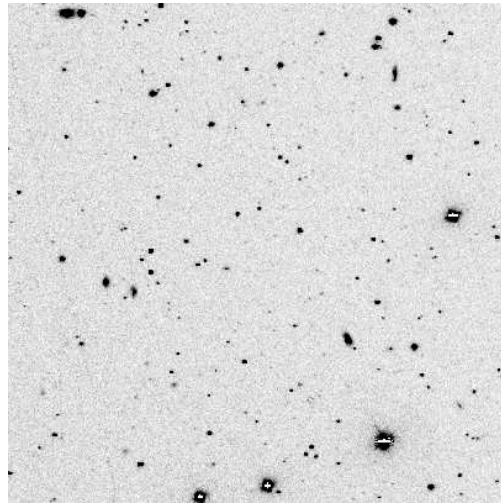


FIG. 2.— An example direct image. This is a small section of the combined (B + V) direct image of survey field F1305. The area shown represents a 512×512 pixel subsection of the total field, or 6.25% of the area of F1305.

(1) *Object location.* It is difficult to assign accurate positions to objects based on their objective-prism spectra. The direct images yield much more accurate positions, and can be used to locate objects that are substantially fainter than are visible in the spectral images.

(2) *Photometry.* The direct images provide accurate B and V magnitudes for all objects in the fields. No follow-up imaging photometry is required.

(3) *Morphology.* Likewise, the direct images are crucial for assessing the nature of candidates in the spectral images. Although the resolution is poor, due to the coarse pixel scale, the images are suitable for object classification (star vs. galaxy) for at least the

brighter objects ($V < 19$).

(4) *Faint ELG detection.* Without the direct images, only objects with a detectable continuum could be selected from the objective-prism images by our automated reduction procedure. Faint ELGs with strong emission lines but weak continua would not be detected, even if the line strengths were well above our detection threshold. By using object locations based on the deeper direct images, even very faint ELGs ($B \approx 21$) can be cataloged.

Spectral Images. At the heart of the KISS project are the objective-prism spectral images. The spectral data acquired for the survey are quite deep, between 1 and 2 magnitudes deeper than previous line-selected

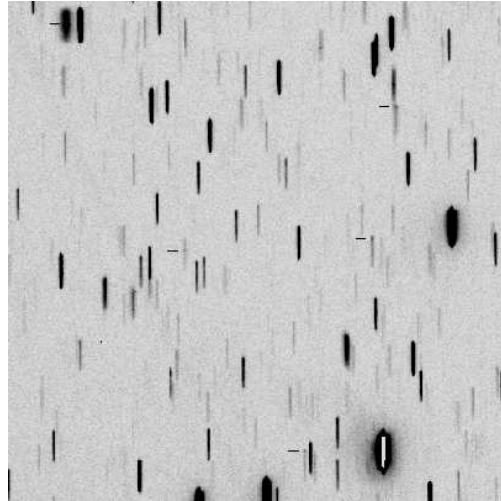


FIG. 3.— An example spectral image. The area shown is the same region depicted in Figure 2, but for the red spectral data. Eight emission-line galaxy candidates located in this field are indicated by the tick marks.

samples like UM, Case, and UCM, and 3 to 4 magnitudes deeper than the Markarian survey data. As mentioned above, spectral data have been obtained for different portions of the first survey strip in one or both of two spectral regions. The blue spectra were obtained for all 102 survey fields, while the red spectra were taken for 54 fields. We began the survey using blue spectra exclusively, with the idea of better matching many of the previous surveys. However, we carried out tests in the red spectral region during our second season of observing, and realized that the combination of higher CCD sensitivity in the red plus the more ubiquitous presence of strong H α (as opposed to [O III]) combined to more than compensate for the higher sky background levels in the red. The net result was a higher detection rate of ELGs per unit area in the red spectra. Hence, after finishing the first survey strip in the blue region, we reobserved as many fields as possible in the red. For all subsequent survey strips, we plan to observe in the red spectral region only, as the red survey detects nearly all (at least 87%) of the objects seen in the blue survey (see Section 4).

Calibration Images. In order to improve observing efficiency, it was decided not to attempt photometric calibration of the direct images on a nightly basis. The key factor driving this decision was the desire to be able to utilize clear but not strictly photometric nights for data acquisition. Hence we developed a scheme of post-calibration, where on just a handful of photometric nights we observed a portion of each field using only the central 512×512 pixels of the CCD. Exposure times were short, the small format images read out in seconds, and accurate positioning was not required. Hence, we could observe a large number of fields in a very short amount of time, interspersing standard star observations throughout. All photo-

metric calibrations were done using standards from Landolt (1992). During the processing of the survey data, the fluxes in the brightest stars in these calibration images were then compared with the fluxes for the same stars in the much deeper survey images, yielding an accurate post-calibration of the main survey images. These calibration images were often obtained during bright time, so that all scheduled dark time could be used for survey work.

2.3. Observing Procedures

We utilized a standardized observing procedure for all data taking. Initial field acquisition was done using setting circles only, since the telescope does not have position encoders. A short test exposure was taken, and the positioning improved by comparing the test image to finder charts (photographic enlargements of the POSS). This was accomplished by moving the telescope by small increments using images displayed on a monitor that are taken with a video camera which is part of the offset-guider system. By careful adjustment, a pointing accuracy of 0.5 to 1 arcmin was achieved. This precision was adequate for our purposes.

Standardized exposure times were used throughout. These times were established early in the project, and reflect a trade-off between our combined goal of good depth and large areal coverage. For observations made in direct mode that were taken early in the project, each field was imaged twice through the V filter for 360 s, and once through the B filter for 720 s. After it was realized that the direct images were substantially deeper than the spectral images (by more than 2 magnitudes), the exposure times for the direct images were reduced to 300 s in V and 600 s in B. The spectral observations consisted of four exposures of 720 s each. Under non-optimal observing

conditions (e.g., a slight haze present, the moon up), these exposure times were increased slightly to compensate, although in general very few images that have been used to construct the survey were taken under these lower-quality conditions. For example, we took almost no survey data while the moon was up, and then only when it was during crescent phase and/or very close to the horizon.

The multiple exposures were acquired in order to allow for the easy removal/rejection of particle events (cosmic rays) in the images. In addition, the telescope was dithered between exposures by \sim 10-15 arc-sec in order to reduce the effect of lower quality regions on the detector (e.g., bad columns, lower sensitivity pixels).

Special care was taken to align the dispersion direction of the prism with the CCD columns when observing in spectroscopic mode. This was accomplished by rotating the prism in its cell until good alignment was achieved. Although not strictly necessary, this step greatly simplifies the procedure of extracting the spectra (see section 3.2).

Calibration data acquired on each night of observing included bias images (zeros) and twilight flats. The twilight flats proved adequate for our purposes, since our program requires flat backgrounds over modest areas of the CCD, but low-level gradients over larger scales could be tolerated. The twilight flats typically produced reduced images that had edge-to-edge gradients of no more than \sim 1%, even for data taken through the prism. We took five twilight flats through each filter, dithering the telescope between exposures. Dark images were taken typically once per run, but as there was no appreciable dark level associated with this CCD, no correction for dark counts was applied.

3. IMAGE PROCESSING

3.1. Preliminary Reductions

As with any major observational survey, image processing and analysis are major components of KISS. One of the primary goals of the KISS project, established during our preliminary discussions about the survey, is to carry out the bulk of the searching and parameter determination for the emission-line galaxy candidates in an automated fashion. To that end, a substantial amount of new software was developed by members of the KISS collaboration. The image processing packages adopted for our work were IRAF⁶ (for the US team) and MIDAS⁷ (for the Russian team). Most of the survey processing and analysis reported here has been done using the IRAF-

based software, a complete description of which is given in Herrero *et al.* (2000). The MIDAS software package is described in Kniazev (1997) and Kniazev *et al.* (1998). In this section we give an overview of the processing steps carried out on the data.

The preliminary processing of the images follow fairly standard procedures. Our first step is to flag the saturated pixels in each image, in order to be able to track them through subsequent analysis steps. This is accomplished by inverting the counts in the saturated pixels (setting pixels with fluxes at 32767 to -32767). Next the bias is removed from each image using a combination of the overscan region (for the mean bias level) and an average of ten bias images (for the 2D bias structure). As mentioned above, no significant dark level is present in the images produced by the CCD, so no dark correction is carried out. The individual twilight flats are combined (using a median combine algorithm) into a single flat-field image, which is then applied to the survey images. Finally, the several bad columns in the S2KA chip are interpolated over to remove the worst of the cosmetic defects of the CCD.

The next stage in the processing involves aligning and combining the individual images of each field into a single, deep combined image. The same procedures are followed for the spectral and direct images. An IRAF script was written as a front-end to the IRAF task `imalign` to expedite the process. This script displays each image in the group in turn, and allows the user to mark stars used to create the rough offsets between the images that are used by `imalign`. Once the images are shifted to a common center, they are combined to create a single, deep image of each field which is fairly free of particle events (although a few invariably survive the process). After the end of the alignment and combining stage, the KISS data consist of a single combined spectral image, a deep combined direct image (created from the two V and one B direct images), a combined V direct image, the single B direct image, plus the small-format calibration images. All three direct images have precisely the same alignment.

Prior to processing the data through the KISS software package, a number of steps are carried out on the images in order to streamline the analysis. These steps are referred to as the pre-KISS processing stage, and amount to converting the data into a uniform format and ensuring that all information necessary for the subsequent KISS processing is present in the image headers. The steps include (1) rotating and/or flipping the images to a standard orientation (N up,

⁶IRAF is distributed by the National Optical Astronomy Observatories, which are operated by AURA, Inc. under cooperative agreement with the National Science Foundation.

⁷MIDAS is an acronym for the European Southern Observatory software package – Munich Image Data Analysis System.

E left); (2) adding certain header keywords that are not placed in the image headers by the acquisition software; (3) computing and inserting into the headers the sidereal time and airmass for the time of the observation; (4) determining accurate central coordinates and field rotation values; (5) measuring the mean FWHM of the stellar point-spread function (PSF) and writing it into the header. For many of the steps, special IRAF scripts have been written to streamline the process. For example, step 4 is carried out using a script which displays an image, overlays the location of all stars in the Guide Star Catalog (GSC, Lasker *et al.* 1990), and allows the user to interactively match objects within the image to their corresponding GSC marker and hence determine the coordinate offset between the field center and the less accurate telescope coordinates. A second stage of the program allows the user to measure and correct for any field rotation present (usually this was no more than 1–2°).

3.2. KISS Package Processing

All subsequent processing and analysis of the KISS data occurs within the KISS software package. This suite of scripts and programs is described in detail in Herrero *et al.* (2000). Here we give a brief summary of the tasks carried out on the data.

The goal of the KISS processing is to extract all useful information from both the direct and spectral images and store it in a conveniently accessible format. For the latter, we adopted the STSDAS Tables format. The first task of the KISS package is therefore the creation of an empty KISS table for each survey field. All relevant information from the image headers is transferred into the table header at this step. Subsequently, all work by the KISS package programs modifies the data contained in the KISS tables, not the images. The processing steps can be conveniently described in terms of seven discrete functions, or modules: (1) object detection and inventory; (2) photometry and object classification; (3) astrometry; (4) spectral image coordinate mapping and background subtraction; (5) spectral extraction and overlap correction; (6) emission line detection; (7) spectral parameter measurement.

(1) *Object Detection and Inventory.* The goal of this module is to locate all objects in the combined direct image with peak fluxes greater than 5 times the local RMS noise (background plus instrumental noise). A series of routines provide for the automatic detection and cataloging of all such objects in each field, plus the facility to interactively reject spurious sources (caused, for example, by diffraction spikes and rings around bright stars) and add ones missed by the automated software. Great care is taken during this

step to ensure a high degree of reliability in the final list of objects in the KISS database for each field. For a typical field, all objects brighter than $V \approx 20.5$ are included. At the end of this stage of processing, the KISS table includes an entry for each detected object. The key information recorded for each object includes an estimate of its brightness and an accurate pixel position (x,y) in the image. An average of 5200 objects are found per field. However, there is a large variation in the number of detected objects within each field, ranging from 3000 to 12000. Most of this variation is due to changing Galactic latitude and longitude.

(2) *Photometry and Classification.* In this second module, the V and B filter images are used along with the small-format calibration images to derive accurate magnitudes and B–V colors for all objects in each field. The multi-aperture photometry is also used to classify the objects brighter than $V = 19$ as either stars or galaxies (see Kearns *et al.* 2000). Objects classified as galaxies are then remeasured using apertures tailored for extended objects. As part of the photometry process, an inventory of nearby sources is created for each object, and those whose photometry is potentially contaminated by near neighbors are flagged in the table. At the end of this stage, each object in the KISS table possesses calibrated B and V magnitudes, a B–V color, and, for the brighter objects, a classification type. Formal errors for all photometric values are also tabulated.

(3) *Astrometry.* Accurate positions for all objects in the KISS table are determined. Stars contained in the GSC are automatically located in each survey field, and a full astrometric solution is obtained and applied to all of the objects in that field. An average of roughly 150 GSC stars are used per field in the solution, and the formal RMS errors in the final positions are typically 0.20–0.25 arcsec in both right ascension and declination.

(4) *Spectral Coordinate Mapping & Background Subtraction.* Once all of the relevant information is gleaned from the direct images, the processing steps begin to focus on the spectral images. The first step involves establishing the coordinate transformation between pixel positions in the direct images and the corresponding positions in objective-prism images. Since the direct images are used exclusively for object identification, we must be able to locate accurately the position of each object in the spectral images based on its direct image coordinates. This is accomplished by an interactive routine that requires the user to provide an initial identification of several objects in both the direct and spectral image. This initial input provides the software with a coarse offset between the two fields, after which many additional

stars are selected automatically, based on brightness, to be used to derive a full two-dimensional coordinate transformation between the two images. This includes terms for the x-y offsets, rotation, and magnification (stretching). Once the transformation is derived, the x-y positions in the spectral image of each object in the KISS table are computed and recorded. Objects which are not completely contained within both the direct and spectral images (i.e., lie entirely or partially off of the edge of one of the two images) are then flagged and removed from the sample. In a subsequent step, the sky background in the spectral image is determined and removed, using a routine that masks each spectrum, then uses the remaining pixels to generate a smoothed, median-filtered background image.

(5) *Spectral Extraction and Overlap Correction.* This module is at the core of the KISS processing. All objects present in the KISS table have their objective-prism spectra extracted into a one-dimensional (1D) format by summing the flux perpendicular to the dispersion direction. Experiments suggested that optimal signal-to-noise is achieved by summing over 4 pixels. The resulting 1D spectra are written to the KISS database table for each object. As part of the extraction process, any spectrum that is overlapped by another is flagged as such by the software, and an algorithm is then applied which attempts to correct for this overlap. The correction uses template 2D spectra generated from isolated bright stars in each field, and makes use of the relative separations and brightnesses of the objects *as measured from the direct images* to determine the proper correction on a pixel-by-pixel basis. This technique successfully corrects for the effects of overlapping spectra in all but the most extreme cases (i.e., those with large brightness differences between the two overlapping objects).

All processing up to this stage is carried out on all objects in each field in a uniform manner. Nothing that occurs prior to this point is specific to the task of detecting emission-line objects. Only at this point, when the KISS table contains complete information about the photometric and astrometric characteristics of each object, as well as the extracted 1D spectra, does the KISS software become specialized to the task of finding ELGs.

(6) *Emission Line Detection.* This module centers upon a non-interactive routine which examines each spectrum for the presence of a strong emission feature. The program fits a low-order polynomial to a median-smoothed version of each spectrum, subtracts the resulting fit from the original spectrum, and then searches for pixels with a flux level above a user-specified threshold. Experimentation with the actual data led us to adopt as our threshold a level

of 5 times the RMS noise in each spectrum. Thus, one should be able to place a high degree of reliability on objects cataloged as ELG candidates. Once the program completes the automated search, all selected candidates are examined visually, both in the objective-prism images and in the extracted spectra. This process usually leads to the rejection of many false detections. The average number of objects found in each field for the red spectral data was 80, of which only 25–30% turned out to be valid ELG candidates. Many of the remaining objects were found to be objects for which the overlap correction was imperfect (e.g., when a very bright object overlaps a faint one), or residual cosmic rays not rejected during the combining step. Each object that passes the inspection stage is flagged in the KISS table as being an ELG candidate.

(7) *Measuring the Spectra.* The final step in the processing involves measuring the spectrum of each of the ELG candidates. A rough wavelength and flux scale is assigned to the objects in each field, and an interactive program displays the spectrum of each ELG candidate and allows the user to measure the putative emission line for both position and total strength. The former is used to estimate the redshift of the galaxy, the latter to estimate the line flux and equivalent width. Although only relatively crude measurements, these quantities provide extremely useful information regarding the survey objects. The accuracy and utility of these measurements is discussed in the following section.

4. RESULTS

The first two lists of KISS ELGs are presented in Salzer et al (2000a, hereafter KB1) for the blue ([O III]-selected) survey and in Salzer et al (2000b, hereafter KR1) for the red (H α -selected) survey. Here, we summarize the main results obtained from these first two survey strips, and give general properties of the survey data. The reader is referred to the two survey papers for complete details regarding the make-up of the ELG candidate lists, the properties of the ELGs, and the estimated completeness of the individual ELG catalogs.

KB1 covers 102 Schmidt fields, aligned in a strip of constant declination ($\delta(1950) = 29^\circ 30'$). The R.A. range covered is $8^h 30^m$ to $17^h 0^m$. This area was chosen to overlap completely the Century Redshift Survey (Geller *et al.* 1997), which provides photometric and redshift information for a sample of 1762 field galaxies complete to $m_R = 16.13$. After accounting for the overlap between the survey fields, the total area covered by KB1 is 116.6 square degrees. A total of 223 ELG candidates were selected for inclusion in the first blue list, which results in a surface density

of 1.91 ELGs per square degree.

The areal coverage of KR1 is substantially less than that of KB1, only 54 Schmidt fields. The red spectral data were taken to overlap with the existing KB1 direct images, so the two surveys cover essentially the same area where they overlap. The R.A. range of KR1 is from $12^h 15^m$ to $17^h 0^m$, excepting the three survey fields between $14^h 30^m$ and $14^h 45^m$. The total area covered by KR1 is 62.2 square degrees, and a total of 1128 ELG candidates are included in this list. The surface density of $\text{H}\alpha$ -selected KISS objects is 18.14 ELGs per square degree! For the area in common between KB1 and KR1, there are 125 blue-selected ELG candidates. Of these, 109 (87%) are also cataloged in KR1, and several of the remaining 16 KB1 candidates not included in KR1 are detected in the red but at levels slightly below our selection threshold. For this reason, coupled with the substantially higher detection rate of the red-selected spectra, all subsequent survey work will be undertaken using red spectra only.

Examples of several newly discovered ELGs are shown in Figures 4 and 5. Figure 4 displays three small sections of a single survey field, showing four KISS ELGs. The objects chosen for this illustration display a range of observational characteristics which reflects the variety seen in the overall survey. These galaxies show a substantial range in brightness, emission-line strength and contrast (equivalent width), and redshift (as indicated by line position). Figure 5 shows plots of the extracted spectra for all four ELGs.

A summary of the previous Schmidt surveys for active galaxies is given in Table 1. This table is not meant to be complete, but rather to give examples of existing surveys for comparison purposes. The surveys listed are grouped by the type of object detection method employed (column 2): color selection, UV-excess selection, emission-line selection, or a combination thereof. Schmidt/objective-prism surveys for QSOs (e.g., PG Survey) are **not** included or discussed here; numbers in the tables for surveys that cataloged both ELGs and QSOs (e.g., UM, Case, Kiso) represent only the galaxies.

All of these surveys, with the exception of KISS, share an important common feature: they were carried out using photographic plates. Even in the era of high quantum efficiency CCD detectors, the large areal coverage of photographic plates has made them the detector of choice for most Schmidt surveys. However, the relatively low sensitivity of the plates has limited the depths of the blue/emission-line galaxy surveys, particularly those which employ an objective prism, since dispersing the light makes the threshold effect of photographic emulsions even

more severe for faint objects.

A few of the surveys listed in Table 1 have utilized scanners to digitize the survey plates, and then used automated detection software to search for emission-line galaxies. These include the Marseille (Surace & Comte 1998) and Hamburg (Popescu *et al.* 1996) surveys, as well as the most recent installment of the UCM survey (Alonso *et al.* 1999). An additional survey of this type that is currently in progress is the Hamburg/SAO survey (Lipovetsky *et al.* 1998, Ugrumov *et al.* 1999), which is similar in most respects to the Hamburg survey.

Two key figures of merit for these surveys are the surface density of objects detected and the completeness limit (or depth). Since objects in a line-selected sample are chosen from the survey images via a complicated combination of emission-line flux and equivalent width (Schmidt *et al.* 1986, Gratton & Osmer 1987, Salzer 1989), it is not possible to compare the depths of these surveys directly with those of the color and UV-excess selected samples, which are effectively magnitude-limited samples (albeit with complex selection functions). *Line-selected surveys can not be treated as magnitude-limited samples.* For comparison purposes only, we include in column (6) of the table the *median blue apparent magnitude* (when available) for some of the line-selected surveys. This should not be taken as anything more than an illustrative number, but it at least allows the various types of surveys to be compared in a rough sense. We stress that one cannot infer accurate relative depths of the various surveys using the numbers in column (6). Still, one does get a feel for the survey depths from these numbers.

The color and UV-excess surveys are all relatively shallow, being complete to only m_B of between 14.8 and 16.0. Some of the line-selected samples appear to be sensitive to much fainter galaxies. The UM survey has a median $m_B = 16.9$, SBS has a median m_B of roughly 17.0, while for the $\text{H}\alpha$ -selected UCM survey, a median blue magnitude of ~ 16.5 is estimated. By comparison, the *median m_B for the $\text{H}\alpha$ -selected KISS galaxies is 18.1*, substantially fainter than the other existing surveys.

Since it is not possible to make a fair comparison between surveys based on their apparent magnitudes, a more relevant value is the surface density of objects. Among the older surveys, those with the highest numbers of objects include the Kiso, SBS, and Case surveys. Kiso is purely color-selected, while the other two use a hybrid selection method, considering both UV-excess and emission lines. Follow-up work on the Case survey (Salzer *et al.* 1995) indicates that, to first order, it can be treated like a color-selected survey, which is why its completeness limit is listed directly.

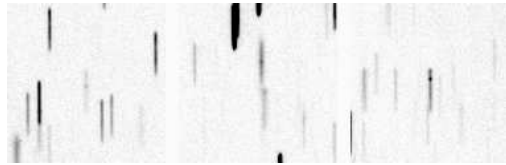


FIG. 4.— Examples of 4 newly discovered ELGs detected in the KISS survey. *Left:* An example of a fairly faint ($B=18.6$) ELG. *Center:* Two ELG candidates: a lower-redshift object just above center, and a high-redshift galaxy just below it. *Right:* An intermediate-redshift object with a fairly strong emission line.

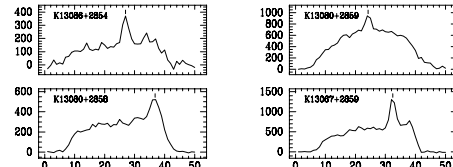


FIG. 5.— Plots of the extracted spectra for the four ELGs displayed in Figure 4. K13086+2854 corresponds to the left image, K13080+2859 (upper) and K13080+2858 (lower) to the center image, and K13067+2859 to the right. Each spectral plot covers ~ 800 Å, in the range 6400 – 7200 Å. Lines mark the location of the $H\alpha$ emission line.

The previous line-selected surveys with the highest surface densities are the UM and UCM surveys, both with roughly one ELG for every two square degrees surveyed. Both of the KISS samples detect objects at a substantially higher rate. The blue, [O III]-selected survey has a density four times higher than the UM survey, with which it compares most directly, and 19 times higher than the famous Markarian survey. The numbers for the red ($H\alpha$ -selected) KISS sample are even more impressive: a factor of 32 times higher surface density than the UCM survey, and 181 times higher than Markarian!

An additional survey that has a number of important similarities to KISS, but that is missing from Table 1, is the Palomar Transit Grism Survey (PTGS, Schneider *et al.* 1994). The reason PTGS is not included in the table is the fact that it is not an objective-prism survey. With that distinction aside, however, PTGS and KISS share a number of attributes. PTGS employed CCDs as their detectors, and hence reached to quite faint magnitudes. Although PTGS was designed primarily to detect high-redshift QSOs, a large fraction of the objects discovered were in fact low-to-moderate redshift galaxies with strong emission lines. The surface density of objects discovered in the two surveys is comparable. Some of the software algorithms developed for KISS were patterned after those first used by PTGS. In particular, we adopted a line-detection algorithm very similar to that used by PTGS (see Herrero *et al.* 2000).

As already mentioned, KISS is the first large-scale survey to utilize CCDs for objective-prism spectroscopy. Other groups have also begun pursuing digital objective-prism survey observations using techniques similar to KISS. These include the QUEST (QUasar Equatorial Survey Team; Sabbe 1999) sur-

vey and the UCM-CIDA survey (Gallego *et al.* 1999).

In the following subsections, we illustrate various properties of the KISS data, including the depth and photometric quality of the direct images, the quality of our positions, and the reliability of the redshift and line-strength information recorded in the survey tables.

4.1. Photometric Quality

The photometric properties of the survey data are conveniently summarized in Figure 6, which shows the data for all objects contained within a single KISS field (F1455). A total of 10,078 objects were detected in this field. The upper panel of the figure shows the histogram of the measured V magnitudes, which peaks at $V \approx 21.0$ ($B \approx 22.0$) and then drops off rapidly at fainter magnitudes. It is likely that many of the very faintest objects found by the software ($V > 22.5$) are spurious sources. These faint objects play no role in the ELG survey, since we do not detect sources this faint in the spectral images. The lower panel in Figure 6 shows the histogram of $B-V$ color for those sources with reasonably reliable photometry (those with $V < 21.5$). The median color is 0.98; clearly this sample of objects is dominated by late type stars. The need for automated software to carry out the survey is clear from these plots: it would be an impossible chore to extract the 15 – 30 ELG candidates from among the 3,000 to 12,000 objects in each field using eye searches alone.

Figure 6b shows the photometric errors associated with the V magnitudes in field F1455. At bright magnitudes, the errors are dominated by uncertainties in the photometric calibration, which are somewhat higher than one might expect due to the “bootstrap” nature of our calibration scheme. The formal errors in our nightly zero-point constants are typically better

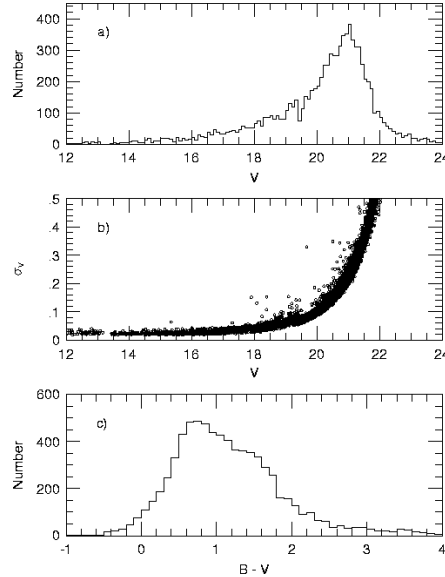


FIG. 6.— (a) Histogram of the V magnitudes for all 10078 objects detected in survey field F1455. The number of objects detected peaks at $V = 21.1$. (b) The formal photometric error (in magnitudes) for all objects detected in field F1455, plotted as a function of V magnitude. (c) Histogram of B-V color for all objects in field F1455 with $V < 21.5$.

than 0.02 magnitude. However, the uncertainty in the photometric offset between the deep survey images and the short-exposure calibration images is usually at about the same level. Hence, for bright objects our photometric precision is typically ± 0.03 -0.04 magnitude. As fainter magnitudes are approached, the sky noise becomes an increasingly important source of uncertainty. To compensate partially for this, fainter objects are measured through progressively smaller apertures, and an aperture correction is applied to the magnitudes. The smallest aperture used is 8 arcsec in diameter, which is used for objects with $V > 19.5$. Beyond this magnitude, the photometric errors increase sharply. For field F1455, a characteristic value of σ_V is 0.10 magnitude at $V = 20.0$, 0.23 magnitude at $V = 21.0$, and 0.36 magnitude at $V = 21.5$.

The depth of the direct images are fairly uniform for the full survey. One way to assess the depth of the imaging data for each field is to measure the peak in the apparent magnitude histogram. When this is done for all 102 fields of KB1, the mean value of $V_{peak} = 20.5$ is determined. This is between one and two magnitudes deeper than the spectral images. The scatter about the mean is 0.25 magnitude, with only four fields having V_{peak} slightly brighter than 20.0. There is no trend in the variation of V_{peak} with position on the sky.

It was difficult to find adequate comparison sources for use in evaluating the quality of the KISS photometry. The survey data yield high quality photometry in the magnitude range $V = 13$ to 20. Brighter than $V = 12$ to 13, stars are saturated in our images. At magnitudes fainter than our saturation limit, most avail-

able photometric data are photographic, and hence not terribly useful in terms of providing a critical test of our precision. One list of fainter stars with published photoelectric photometry which overlaps our survey area is given in Purgathofer (1969). This list of 33 stars is contained within our F1305 survey field, and includes stars with a brightness range of $V = 12.8$ to 18.5. Comparison of the KISS photometry with that published by Purgathofer shows good agreement. The mean offset in V between the two datasets is -0.001, with a scatter of 0.039 magnitude. This level of scatter is fully consistent with the formal errors in the KISS photometry. Similar agreement is found for the B photometry, although the mean offset between the two data sets of $\Delta B = 0.043$ is marginally significant. Further work will be required to better assess the reality of this offset. It would appear, however, that there are no large (> 0.05 magnitude) photometric offsets in our data, at least for magnitudes brighter than 18.5.

4.2. Astrometric Quality

A goal of the project is to provide sub-arcsecond precision in our astrometry. This motivation is driven in a large part by our expectation that follow-up spectra would be most efficiently obtained using multi-fiber spectrographs (e.g., Hydra at Kitt Peak), and accurate positions are a prerequisite for such instruments. For this reason, a full astrometric solution is obtained for each survey field, using the Guide Star Catalog (Lasker *et al.* 1990) as our source for positions.

An internal estimate of our positional accuracy is provided by our own astrometry routine, which after

computing the astrometric solution for a given field compares the final calculated positions of the GSC stars with their cataloged values. The average value of the RMS scatter between the calculated and catalog positions for the 102 KISS fields is 0.25 arcsec in R.A. and 0.20 arcsec in declination. Given our image scale of 2.03 arcsec/pixel, we are satisfied with this level of precision. These values represent the typical *relative* positional accuracy for objects within a given field, a number which is relevant when considering the positional precision that is necessary when using a multi-fiber spectrograph.

The estimate of the absolute precision of our positions was obtained by comparing our astrometry with that of Willmer *et al.* (1996), who performed detailed astrometric solutions for photographic plates as part of a deep survey for galaxies in the North Galactic Pole. Four of the KISS fields overlap parts of the Willmer *et al.* survey. We matched the stellar sources in Willmer *et al.* with their corresponding objects in the KISS database, and computed the mean positional offsets between the two catalogs for the 695 stars in common. The range of magnitudes covered by the stars in this overlap sample was 11.0 – 15.5. The average difference in R.A. (in the sense KISS – Willmer) was 0.71 arcsec, with individual fields having offsets as large as 1.06 arcsec and as small as 0.35 arcsec. Positional agreement in declination was somewhat better, with an average difference (again, KISS – Willmer) of 0.29 arcsec and a range of 0.07 to 0.46 for individual fields. The differences between the two samples are most likely due to the different sources of astrometric materials used by the two surveys. Willmer *et al.* used an astrometric catalog from the Lick Astrograph, and showed that there are irregularities with the GSC at the level found here. We conclude that the *absolute* astrometric precision of KISS is limited by the precision of the GSC, but is probably better than 1 arcsec for most fields. There is no indication of errors as large as 2 arcsec. However, we point out that this detailed comparison was carried out over a limited area of the overall survey.

4.3. Morphology

The KISS direct images have a rather coarse scale of 2.03 arcsec/pixel. This makes detailed morphological analysis difficult for objects fainter than $V \approx 19$. For brighter objects, the KISS software package provides automated object type classification. At this time, the classification is limited to a simple star vs. galaxy designation. The distinction between the two classes of objects is important, however, since various KISS routines make use of the object type classification in order to provide better results. For example, those objects flagged as galaxies are repho-

tometered with appropriately sized apertures, since the main photometry routine uses apertures tuned to stellar sources. The emission-line detection routine also makes use of the object classification to help eliminate the many false detections that occur for late type stars. Stars of spectral type M have objective-prism spectra which mimic those of ELGs in the red spectral region. Our software automatically rejects objects classified as stars that have colors redder than $B-V = 1.30$.

The automated classification has the added advantage that we can use the KISS imaging data to produce a digital galaxy catalog for the area covered by the survey. This catalog includes accurate B and V photometry to $V = 19.0$. Kearns *et al.* (2000) details the use of the object classification software to produce such a galaxy catalog, and then uses the catalog to do a number count analysis (see Section 5).

4.4. Confirmation of ELG Status

Beginning in 1998, follow-up spectra of candidate KISS ELGs were obtained using both multi-fiber and single-slit spectrographs. During our first two seasons of spectroscopic follow-up, 428 candidates from KR1 were observed. Of these, 402 (94%) were confirmed to be *bona fide* ELGs. Of the 26 unconfirmed KISS objects, 16 were found to be Galactic stars, while 10 were galaxies without significant emission. Inspection of the original objective-prism data for these unconfirmed objects reveals that they were in all cases “dubious” candidates, in the sense that the apparent emission line was questionable. In all cases, the putative line turned out to be either noise (e.g., a remnant cosmic ray) or an artifact of two overlapping spectra. The results of our follow-up spectra will be valuable in helping to fine tune the selection process for subsequent survey lists.

A complete description of the follow-up spectroscopy obtained to date for the KISS ELG sample is given in Gronwall *et al.* (2000b).

4.5. Redshift Comparison

One of the parameters we measure directly from the survey data is the redshift of each ELG. The assumption made is that the line observed in the objective-prism spectrum is either $H\alpha$ (for red spectra) or $[O\ III]$ (for blue spectra). To date, only ELG candidates from KR1 have been observed spectroscopically, so the results discussed here and in the following subsection refer only to the red survey, and the detected line is assumed to be $H\alpha$. This is usually a good assumption: of the 402 confirmed ELGs from the follow-up spectra mentioned above, only eight (2%) are high redshift objects where $[O\ III]$, $H\beta$, or, in one case, $H\gamma$, is shifted into the spectral region

covered by our red spectra. Seven of the eight are AGNs, with redshifts between 0.328 and 0.550. In all other cases, the observed emission line was in fact H α . Given this result, we were interested in determining the level of precision in our redshifts estimated from the survey data.

Figure 7 shows a direct comparison of survey and slit-spectra redshifts for all objects with follow-up spectra (excluding the high-z objects). A very tight, linear correlation is seen. For redshifts up to $z \approx 0.07$, the KISS redshift is seen to be an excellent predictor of the true redshift. The RMS scatter about the line $z_{KISS} = z_{slit}$ is only 0.0028 (830 km s $^{-1}$) for $z_{slit} < 0.07$. This number is consistent with expectations based on the value of the dispersion provided by the prism. We consider this level of redshift precision to be excellent, and allows us to use the survey data themselves for certain types of analyses (see Section 5).

At higher redshifts, z_{KISS} is seen to underestimate the true redshift by a modest amount. This is due to the steep cut-off of the survey filter. As the H α line redshifts into the wavelength region where the filter transmission drops off sharply, the red side of the emission line is reduced in strength, which pushes the flux-weighted line centroid to lower wavelengths (and hence lower redshifts). A correction for this effect can be obtained by fitting the residuals in Figure 7 at $z_{slit} > 0.07$ and applying the resulting correction to the high-z portion of the KISS sample. An example of a linear correction fit is shown as a dashed line in the figure.

One additional comparison that we can make in terms of the redshift precision is with KISS galaxies which are also members of the UCM survey. Comparison of the KR1 list with the UCM objects observed by Gallego *et al.* (1996) shows that there are 17 objects in common. The mean redshift difference for these galaxies (in the sense $z_{UCM} - z_{KISS}$) is $\Delta z = -0.00012$ (-35 km s $^{-1}$), while the RMS scatter is 0.0030 (900 km s $^{-1}$). Once again, we see that the objective-prism redshifts provide reasonable estimates of the true redshifts, although of limited precision.

4.6. Line Flux and EW Comparison

The line fluxes and equivalent widths (EWs) measured directly from the objective-prism spectra are extremely valuable for establishing the completeness limits of the survey. In addition, the H α fluxes from the red survey, if reliably calibrated, can be used to estimate the total star-formation rate of each KISS galaxy without the need for follow-up spectroscopy (e.g., Gronwall 1999).

The line fluxes are calibrated in a two-step process. First, the spectra from all of the survey fields

are placed on the same flux scale by comparing the observed fluxes from a sample of stars selected to fall within a narrow range of color and apparent magnitude. This procedure corrects the data from each field for overall throughput variations, and ensures that the fluxes from the objective-prism data can be compared directly. The absolute flux calibration of the H α line is achieved using follow-up spectra obtained with slit spectrographs. We found that spectra obtained through fiber-fed spectrographs systematically underestimate the true H α flux, hence we only used spectra obtained on photometric nights through modest slit widths (typically 2 arcsec) to calibrate the objective-prism fluxes. Details of the flux calibration are given in KR1.

To assess the accuracy of our flux calibration using an independent dataset, we compare our objective-prism measured line strengths against the slit spectra of Gallego *et al.* (1996) for the objects in common. Since our objective-prism spectra are of such low dispersion, the [N II] $\lambda\lambda 6548, 6583$ doublet is always blended with H α . Thus any measured line flux and equivalent width is really H α plus [N II]. For this reason, we plot in Figure 8 the Gallego *et al.* H α + [N II] fluxes vs. the KISS objective-prism line fluxes. There is extremely good agreement between the two datasets, although a few discrepant sources are evident. Two of the deviant objects lie below the $F_{UCM} = F_{KISS}$ line, suggesting that the flux measured by Gallego *et al.* may be underestimating the total H α emission for these objects. This would be the case if the emission were more extended than the width of the slit used by Gallego *et al.*, which appears to be true for both galaxies. The deviant point at the top of the plot most likely represents a case of the KISS flux being underestimated. This object (designated UCM 1259+2934) has a bright neighboring galaxy, for which an overlap correction was applied (see Section 3.2 and Herrero *et al.* 2000). Presumably the objective-prism flux was inappropriately reduced by this correction. In general, however, the KISS fluxes agree well with fluxes derived from slit spectra when the emission region is unresolved. For extended emission, the KISS spectra recover more of the total emission than do slit (or fiber-fed) spectra. Hence, despite being rather coarse in nature, the KISS spectra may be the dataset of choice for use in deriving parameters such as the total star-formation rate for this sample of galaxies.

5. USES OF THE SURVEY

KISS provides a very deep, statistically complete sample of active and star-forming galaxies. A huge advantage over most previous objective-prism surveys is that the completeness limits and selection function

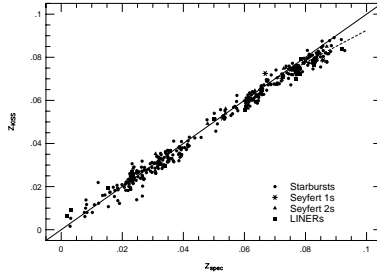


FIG. 7.— Redshifts determined from the objective-prism spectra are compared to redshifts determined from follow-up spectra for 394 KISS ELGs. Galaxies of different types are plotted with the symbols shown in the legend. The solid line indicates $z_{KISS} = z_{spec}$; it is not a fit. The dashed line is a fit to the galaxies with $z_{spec} > 0.07$, where the onset of the survey filter cutoff results in a systematic underestimation of the redshift by the KISS spectra.

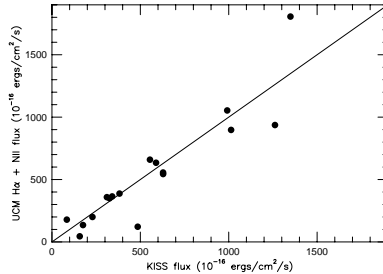


FIG. 8.— Comparison of the $H\alpha + [N\text{ II}]$ line fluxes and KISS objective-prism fluxes for galaxies observed by Gallego *et al.* 1996 that are common to both the KISS and UCM surveys. The solid line denotes $F_{KISS} = F_{UCM}$.

of KISS can be quantified from the survey data themselves. Such a sample can be used to study a wide range of problems in modern astrophysics. In this section we briefly discuss a number of possible applications of the KISS sample. The list can be broken up into four broad categories.

Galaxian Properties / Galaxy Evolution.

The KISS galaxies should provide an excellent catalog for addressing a number of issues regarding the properties of star-forming and active galaxies, particularly the types of questions that require statistically complete datasets. For example, KISS should yield accurate numbers for the frequency of AGN/starburst activity within the general galaxian population. Once follow-up spectra have been obtained for large enough samples of the KISS ELGs, studies of the characteristics of the large-scale star-formation processes occurring in galaxies, the chemical enrichment/evolution in galaxies (particularly dwarfs), and the verification/quantification of a metallicity–luminosity relationship for starbursting galaxies will all be possible.

Another study that should yield fruitful results will be to correlate the KISS catalog of ELGs with surveys at other wavelengths, such as the radio, FIR, and X-ray. Since KISS is so deep, it will match up well with a number of recent surveys. These multi-wavelength studies of the KISS sample should lead

to new insights into the nature of the activity present in these galaxies. The first stages of a correlation between the FIRST radio survey (Becker *et al.* 1995) and KISS (the FIRST–KISS project) is already underway (Beckerman *et al.* 1999), and a complementary project involving the IRAS survey database is planned.

Activity in Galaxies. The KISS survey will provide a deep, complete sample of AGN which will be a valuable complement to existing samples of radio and X-ray selected Seyferts. One clear advantage of KISS over previous objective-prism surveys is that the $H\alpha$ selection method means that a more complete sample of nearby AGN will be detected. For example, the $H\alpha$ -selected portion of KISS is sensitive to LINERS (Heckman 1980), while the older $[O\text{ III}]$ -selected samples such as UM, Tololo, and Case are not. Also, the $H\alpha$ -selected sample appears to detect a much larger fraction of Seyfert 2 galaxies than previous surveys which were carried out in the blue. This is because Seyfert 2s are typically more heavily reddened than Seyfert 1 galaxies. One of the interesting topics that could be investigated is the study of the active stages of galaxian evolution. In particular, what fraction of the local galaxy population currently host an active nucleus? Or, assuming that all large galaxies contain a central black hole, what fraction of the time

are the nuclei “turned on”? Other areas of interest, particularly once follow-up spectra are available, will be the physics of AGN/QSO phenomena with an emphasis on testing the unified model, the environmental influences on activity, and similarities/differences between AGN selected at optical, radio, and X-ray wavelengths.

Observational Cosmology. The KISS survey has the potential to contribute a great deal in the area of observational cosmology. For example, pre-selecting galaxies that exhibit strong optical emission lines is an efficient way to carry out redshift survey work to probe large-scale structure (e.g, Salzer 1989; Rosenberg *et al.* 1994). The surface density of the survey is sufficiently high (e.g., comparable to the Century Survey of Geller *et al.* (1997)) that KISS-selected galaxies could quickly map out the spatial distribution of field galaxies to $z \sim 0.095$ in the areas surveyed. Further, line-selected samples of galaxies, such as the KISS, Tololo, UM, and UCM surveys, tend to preferentially detect dwarf galaxies (Salzer 1989). Studies of the spatial distribution of dwarfs (e.g., Salzer & Rosenberg 1994, Pustil’nik *et al.* 1995, Popescu *et al.* 1997, Telles & Maddox 1999, Lee *et al.* 2000), made possible with dwarf-rich samples such as these, will allow for the study of biasing in the spatial distribution of low-mass galaxies. Our preliminary analysis indicates a significant population of dwarf galaxies within nearby voids. A detailed discussion of both of these issues appears in Lee, Salzer & Gronwall (2000).

An important set of observables from the very early universe are the abundances of the primordial elements (e.g., He, D, Li). Key among these is helium. By studying low metallicity galaxies (i.e., those with relatively little chemical processing since their formation), astronomers have tried to infer the primordial abundance of helium, Y_P (e.g., Izotov & Thuan 1998). This has been an active area of research for some time, yet there continues to be substantial debate over the correct value of Y_P . The effort to determine Y_P accurately would be aided by the existence of a larger sample of very metal poor galaxies. However, despite focused efforts to discover ultra-low metallicity objects ($Z < Z_\odot/25$, see Kunth & Sargent 1986), very few such objects are known. Ideal candidates for this work would possess strong emission lines, to facilitate the abundance determination. Further, they would tend to have weak oxygen lines, due to their low metallicity. The focus of previous searches on the contents of the [O III]-selected photographic surveys may then have created a huge bias against finding more low- Z galaxies. Selecting by $H\alpha$, as KISS does, may well lead to the discovery of many previously unidentified low metallicity galax-

ies with which to investigate the primordial helium abundance.

Finally, the KISS sample will be useful as a low-redshift comparison group to the galaxian population at higher redshift. Understanding adequately the activity levels seen in high- z samples of galaxies that are currently being studied using 10-meter class ground-based telescopes and HST will require having a much better knowledge of the galaxian population locally. Because we can quantify the completeness limits of KISS, it will be an excellent sample to use for comparisons to higher redshift surveys. We will be able to measure more accurately than ever before the space densities of starbursting galaxies locally, which may well have an impact on resolving the faint blue galaxy problem. In addition, KISS will also provide a more accurate estimate of the local star-formation rate (SFR) density (e.g., Gallego *et al.* 1995; Madau *et al.* 1998) which, when combined with high-redshift studies, will lead to a more precise understanding of the evolution of the SFR as a function of cosmic epoch. A preliminary effort to determine the local SFR density using the KISS galaxies is given in Gronwall (1999). A more complete analysis is in progress (Gronwall *et al.* 2000a).

Surveys for Other Types of Objects. As stressed in Section 3.2, the processing and analysis of the KISS data is completely general, up to the stage of searching for emission lines. Therefore, the information tabulated in the survey database files can easily be utilized for surveys of other types of objects. The only restriction is that the type of object being searched for would need to have an identifiable spectral feature in the bandpass of the KISS objective-prism spectra. Although the restricted wavelength coverage of the KISS spectra limits the type of objects one can search for, there is nonetheless potential for these data beyond their primary purpose for KISS.

One such use that was explored was to employ the blue spectral data to look for carbon stars (C stars). The deep absorption band at $\lambda \approx 5150$ Å was targeted. The KISS package routine for detecting the emission lines in the extracted spectra was replaced by a similar routine that examined the spectra of red objects ($B - V > 1.2$) for the presence of a strong absorption feature at the correct location. A list of ~ 75 C star candidates was generated for the 117 square degrees of the blue survey. Spectroscopic follow-up observations have been obtained for roughly a third of these candidates. All three previously known C stars in this area of the sky were recovered. However, none of the other objects for which we obtained higher dispersion spectra have turned out to be C stars. Rather, they are all late-type stars with spec-

tral types of K and M. Apparently, the KISS spectra are not sensitive enough to substantially improve upon the existing surveys for C stars. Despite this result, we will continue to look for additional opportunities to utilize the KISS data for the detection and cataloging of other types of objects.

Another project that is currently underway, for the purpose of doing galaxian number counts, is the development of a digital catalog of galaxies that is complete to $B \approx 20$. While ultra-deep number counts have been carried out with CCDs for years in small areas of the sky, the number counts at brighter levels ($B = 14 - 19$) have either made use of photographic plates (and suffered from questionable photometry) or used CCDs but covered only relatively small areas ($\lesssim 10 \text{ deg}^2$). Currently, KISS direct images exist for over 200 deg^2 and possess well-calibrated photometry. Our galaxy catalog should provide some of the best available number count data in the magnitude range indicated above, since it covers a large enough area to average over localized variations in the large-scale structure. Kearns *et al.* (2000) presents the initial results of this project. In addition, Kearns is also currently investigating the use of the KISS direct images to generate catalogs of low-surface-brightness galaxies.

6. SUMMARY

We have presented a description of the KPNO International Spectroscopic Survey (KISS), a new objective-prism survey for extragalactic emission-line objects. KISS is the first large survey to combine CCD detectors with the traditional Schmidt telescope slitless-spectroscopic-survey method, which has proven to be extremely fruitful over the past three decades. The superior sensitivity of the CCD allows us to survey to fainter flux levels than were previously possible using photographic plates. In addition, the digital nature of the data will allow us to assess the selection function and completeness limits of the survey far more accurately than with photographic surveys.

KISS is being carried out on the Burrell Schmidt telescope. The first survey region was observed in both the red and blue spectral regions. Both sets of objective-prism spectra were obtained over a restricted wavelength region in order to minimize the problems of overlapping spectra and to reduce the level of the sky background. The blue spectral region covers 4800 - 5500 Å, and the primary emission line we select by is $[\text{O III}]\lambda 5007$. The red spectra cover the wavelength range from 6400 - 7200 Å, and objects are detected primarily via the $\text{H}\alpha$ line. Both the red and the blue spectra detect galaxies out to $z \approx 0.095$ via the primary line, and are sensitive to higher- z galaxies over restricted redshift intervals as

other lines move into the survey bandpasses.

Because of the digital nature of the survey data, all of the candidate selection is carried out using automated software, although the final candidate lists are also checked visually. In addition to the objective-prism spectra used to select the ELG candidates, we also have direct images taken through B and V filters which provide accurate astrometry, photometry, and morphological information for all objects in each field. These data, plus estimates of the redshift and line flux for each ELG candidate obtained from the objective-prism spectra, yield a fairly complete picture of each candidate galaxy without the need for additional follow-up observations. This makes the KISS database particularly valuable for statistical studies of galaxian activity.

The results obtained from our first survey lists are extremely encouraging. The first blue survey strip covers 117 deg^2 and includes 223 cataloged ELG candidates. With a surface density of just under 2 ELGs per square degree, the blue KISS sample is substantially deeper than previous surveys of this type. The numbers for the $\text{H}\alpha$ (red) survey are even more impressive. A total of 1128 ELGs have been found in an area of 62 deg^2 , for a surface density of 18.1 ELGs per square degree. This is 32 times the surface density of the $\text{H}\alpha$ -selected UCM survey, and 181 times that of the UV-excess Markarian survey.

The first two survey lists will be presented in Salzer *et al.* (2000a,b), along with a complete discussion of the characteristics of the two samples. Additional survey lists will be published as the data are acquired, processed, and cataloged. To date, data covering 200 deg^2 of sky have been obtained, and observations are continuing. Our overall project goal is to cover in excess of 300 deg^2 in a series of survey strips in selected areas of both the north and south Galactic caps. This will yield several thousand ELG candidates, which will be suitable for addressing a wide range of scientific questions that cover nearly the full scope of extragalactic astronomy.

We gratefully acknowledge financial support for the KISS project through NSF Presidential Faculty Award to JJS (NSF-AST-9553020), which was instrumental in allowing for the international collaboration. Additional support for this project came from NSF grant AST-9616863 to TXT, and from Kitt Peak National Observatory, which purchased the special filters used by KISS. The following summer research students working at Wesleyan University, and supported by the Keck Northeast Astronomy Consortium student exchange program, made major contributions to the survey: Michael Santos, Laura Brenneman, Erin Condy, and Kerrie McKinstry. In ad-

dition, Wesleyan University students Scott Randall, Nick Harrison, Katherine Rhode, Karen Kinemuchi, Kristin Kearns, Eli Beckerman, and Janice Lee, plus Cheshire (CT) High School teacher Julie Barker, worked on various aspects of the survey. Without the participation of all these dedicated young scientists, this work would not have been as successful. We are grateful to Vicki Sarajedini, who assisted in so many ways during the final production of this paper. We thank Bruce Margon and Eric Deutsch for collaborating on the carbon star project, including obtaining spectra for several of the candidates. We also thank the numerous colleagues with whom we have discussed the KISS project over the past several years, including Jesus Gallego, Rafael Guzman,

David Koo, and Danial Kunth. Helpful suggestions made by an anonymous referee are acknowledged with gratitude. Finally, we wish to thank the support staff of Kitt Peak National Observatory for maintaining the telescope and instrument during the early years of the project, and the Astronomy Department of Case Western Reserve University for taking over this role after 1997. In particular, special thanks to Bill Schoening, whose dedication has enabled so much useful science to come out of the Burrell Schmidt, and to Heather Morrison and Paul Harding, who have ensured that the telescope will continue to provide excellent science for years to come.

The KPNO International Spectroscopic Survey is dedicated to the memory of Valentin Lipovetsky.

REFERENCES

Alonso, O., García-Dabó, C. E., Zamorano, J., Gallego, J., & Rego, M. 1999, *ApJS*, 122, 415

Armandroff, T. E. 1995, in *IAU Colloquium No. 148: The Future Utilization of Schmidt Telescopes*, ed. J. Chapman, R. Cannon, S. Harrison, and B. Hidayat (ASP, San Francisco), p. 21

Becker, R. H., White, R. L., & Helfand, D. J. 1995, *ApJ*, 450, 559

Beckerman, E., Salzer, J. J., Gronwall, C., & Frattare, L. M. 1999, *BAAS*, 31, 827

Coziol, R., Demers, S., Barnéoud, R., & Peña, M. 1997, *AJ*, 113, 1548

Coziol, R., Demers, S., Peña, M., Torres-Peimbert, S., Fontaine, G., Wesemael, F., & Lamontagne, R. 1993, *AJ*, 105, 35

Gallego, J., Zamorano, J., Aragón-Salamanca, A., & Rego, M. 1995, *ApJ*, 455, L1

Gallego, J., Zamorano, J., Rego, M., Alonso, O., & Vitores, A.G. 1996, *A&AS*, 120, 323

Gallego, J., Bruzual, A. G., Garcíá-Dabó, C. E., Bongiovanni, A., & Rego, M. 1999, in *Galaxies at high redshift: XI Canary Islands Winter School on Astrophysics*, eds: F. Sanchez, I. Perez-Fournon, M. Balcells, (Cambridge University Press), in press

Geller, M. J., Kurtz, M. J., Wegner, G., Thorstensen, J. R., Fabricant, D. G., Marzke, R. O., Huchra, J. P., Schild, R. E., & Falco, E. E. 1997, *AJ*, 114, 2205

Gratton, R. G., & Osmer, P. S. 1987, *PASP*, 99, 899

Green, R. F., Schmidt, M., & Liebert, J. 1986, *ApJS*, 61, 305

Gregory, S. A., Tifft, W. G., Moody, J. W., Newberry, M. V., & Hall, S. M. 2000, *AJ*, 119, in press

Gronwall, C. 1999, in *After the Dark Ages: When Galaxies were Young (The Universe at 2 < z < 5)*, eds. S. Holt & E. Smith (American Institute of Physics), p. 335

Gronwall, C., Condy, E., Brenneman, L., Santos, M., & Salzer, J. J. 2000a, in preparation

Gronwall, C., Salzer, J. J., McKinstry, K., Wegner, G. 2000b, in preparation

Haro, G. 1956, *Bol. Obs. Tonantzintla y Tacubaya*, 2, 8

Heckman, T. M. 1980, *A&A*, 87, 152

Herrero, J. L., Frattare, L. M., Salzer, J. J., Gronwall, C., & Kearns, K. 2000, submitted

Izotov, Y. I. & Thuan, T. X. 1998, *ApJ*, 500, 188

Kearns, K., Gronwall, C., & Salzer, J. J. 2000, in preparation

Kniazev, A. Y. 1997, Ph.D. Thesis, Special Astrophysical Observatory, Nizhnij Arkhys

Kniazev, A., Salzer, J., Lipovetsky, V., Boroson, T., Moody, J., Thuan, T., Izotov, Yu., Herrero, J., & Frattare, L. 1998, in *I.A.U. Symposium No. 179: New Horizons from Wide-Field Imaging*, eds. B. J. McLean, D. A. Golombek, J. J. Hayes, and H. E. Payne. (Kluwer), p 302

Kunth, D., & Sargent, W. L. W. 1986, *ApJ*, 300, 496

Kunth, D., Sargent, W. L. W., & Kowal, C. 1981, *A&A*, 44, 229

Landolt, A. U. 1992, *AJ*, 104, 340

Lasker, B. M., Sturch, C. R., McLean, B. J., Russell, J. L., Jenkner, H., & Shara, M. M. 1990, *AJ*, 99, 2019

Lee, J. C., Salzer, J. J., & Gronwall, C. 2000, *ApJ*, in preparation

Lee, J. C., Salzer, J. J., Law, D. A., & Rosenberg, J. L. 2000, *ApJ*, in press

Lipovetsky, V., Engels, D., Ugrumov, A., Hopp, U., Richter, G., Izotov, Y., Kniazev, A., & Popescu, C. 1998, in *I.A.U. Symposium No. 179: New Horizons from Wide-Field Imaging*, eds. B. J. McLean, D. A. Golombek, J. J. Hayes, and H. E. Payne. (Kluwer), p 299

MacAlpine, G. M., Smith, S. B., & Lewis, D. W. 1977, *ApJS*, 34, 95

MacAlpine, G. M., & Williams, G. A. 1981, *ApJS*, 45, 113

Macdua, P., Pozzetti, L., & Dickinson, M. 1998, *ApJ*, 498, 106

Markarian, B. E. 1967, *Astrofizika*, 3, 55

Markarian, B. E., Lipovetskii, V. A., & Stepanian, D. A. 1981, *Astrofizika*, 17, 619

Markarian, B. E., Lipovetskii, V. A., & Stepanian, D. A. 1983, *Astrofizika*, 19, 29

Markarian, B. E., & Stepanian, D. A. 1983, *Astrofizika*, 19, 639

Pesch, P., & Sanduleak, N. 1983, *ApJS*, 51, 171

Popescu, C. C., Hopp, U., & Elsässer, H. 1997, *A&A*, 328, 756

Popescu, C. C., Hopp, U., Hagen, H. J., & Elsässer, H. 1996, *A&AS*, 116, 43

Purgathofer, A. T. 1969, *Bull. Lowell Obs.*, No. 147, 98

Pustil'nik, S., Ugrumov, A. V., Lipovetsky, V. A., Thuan, T. X., Guseva, N. 1995, *ApJ*, 443, 499

Rosenberg, J. L., Salzer, J. J., & Moody, J. W. 1994, *AJ*, 108, 1557

Sabbey, C. N. 1999, Ph.D. thesis, Yale University

Salzer, J. J. 1989, *ApJ*, 347, 152

Salzer, J. J., Gronwall, C., Lipovetsky, V. A., Kniazev, A., Sarajedini, V. L., Moody, J. W., Boroson, T. A., Thuan, T. X., Izotov, Y. I., Herrero, J. L., & Frattare, L. M. 2000a, in preparation (KB1)

Salzer, J. J., Gronwall, C., Lipovetsky, V. A., Kniazev, A., Moody, J. W., Boroson, T. A., Thuan, T. X., Izotov, Y. I., Herrero, J. L., & Frattare, L. M. 2000b, in preparation (KR1)

Salzer, J. J., Moody, J. W., Rosenberg, J. L., Gregory, S. A., & Newberry, M. V. 1995, *AJ*, 109, 2376

Salzer, J. J., & Rosenberg, J. L. 1994, in *Dwarf Galaxies*, ed. G. Meylan and P. Prugniel (ESO: Garching bei München), p. 129

Schmidt, M., Schneider, D. P., & Gunn, J. E. 1986, *ApJ*, 306, 411

Schneider, D. P., Schmidt, M., & Gunn, J. E. 1994, *AJ*, 107, 1245

Smith, M. G. 1975, *ApJ*, 202, 591

Smith, M. G., Aguirre, C., & Zemelman, M. 1976, *ApJS*, 32, 217

Stepanian, J. A. 1994, Doctoral Dissertation, Nizhnij Arkhys

Stephenson, C. B., Pesch, P., & MacConnell, D. J. 1992, *ApJS*, 82, 471

Surace, C., & Comte, G. 1998, *A&AS*, 133, 171

Takase, B., & Miyauchi-Isobe, N. 1993, *Publ. Nat. Astron. Obs. Japan*, 3, 21

Telles, E. & Maddox, S. 1999, *MNRAS*, in press

Ugryumov, A. V., Engels, D., Lipovetsky, V. A., Hagen, H.-J., Hopp, U., Pustilnik, S. A., Kniazev, A. Y., Richter, G., Izotov, Y. I., & Popescu, C. C. 1999, *A&AS*, 135, 511

Wamsteker, W., Prieto, A., Vitores, A., Schuster, H.E., Danks, A.C., González, R., & Rodríguez, G. 1985, *A&AS*, 62, 255

Wasilewski, A. J. 1983, *ApJ*, 272, 68

Willmer, C. N. A., Koo, D. C., Ellman, N., Kurtz, M. J., & Szalay, A. S. 1996, *ApJS*, 104, 199

Zamorano, J., Gallego, J., Rego, M., Vitores, A. G., Alonso, O. 1996, *ApJS*, 105, 343

Zamorano, J., Rego, M., Gallego, J., Vitores, A. G., González-Riestra, R., & Rodríguez-Caderot, G. 1994, *ApJS*, 95, 387

TABLE 1
PARTIAL LIST OF PREVIOUS SCHMIDT/OBJECTIVE-PRISM SURVEYS

Survey Name (1)	Type ^a (2)	Area (deg. ²) (3)	Number of objects (4)	Density (# / deg. ²) (5)	Completeness ^b Limit (m _B) (6)	Ref. (7)
Haro	C	Lots	~40	small	??	1
Kiso	C	5100	8162	1.60	16.0	2
Montreal	C	4400	469	0.11	14.8	3
Markarian	UV	15000	1500	0.10	15.2	4
Tololo	L	1225	201	0.16	—	5
UM	L	667	349	0.52	(16.9)	6
Wasilewski	L	825	96	0.18	(15.2)	7
POX	L	82	23	0.28	(16.0)	8
ESO - H α	L	400	113	0.28	—	9
UCM	L	471	263	0.56	(~16.5)	10
Hamburg	L	1248	196	0.16	—	11
Marseille	L	46.5	92	1.98	(~16.0)	12
Case	UV + L	1440	1551	0.94	16.0	13
SBS	UV + L	~990	~1300	1.31	(~17.0)	14
KISS - red	L	62.2	1128	18.14	(18.1)	15
KISS - blue	L	116.6	223	1.91	(18.2)	15

^a C = Color Selected; UV = UV Excess Selected; L = Line Selected

^b Values in parentheses are median apparent magnitudes for that survey, not a completeness limit.

REFERENCES.—1 = Haro 1956; 2 = Takase & Miyauchi-Isobe 1983; 3 = Coziol *et al.* 1993, 1997; 4 = Markarian 1967, Markarian, Lipovetskii & Stepanian 1981; 5 = Smith 1975, Smith, Aguirre & Zemelman 1976; 6 = MacAlpine, Smith & Lewis 1977, MacAlpine & Williams 1981; 7 = Wasilewski 1983; 8 = Kunth, Sargent & Kowal 1981; 9 = Wamsteker *et al.* 1985; 10 = Zamorano *et al.* 1994, 1996; 11 = Popescu *et al.* 1996; 12 = Surace & Comte 1998; 13 = Pesch & Sanduleak 1983, Stephenson, Pesch, & MacConnell 1992; 14 = Markarian *et al.* 1983, Markarian & Stepanian 1983, Stepanian 1994; 15 = this paper, Salzer *et al.* 2000a,b